EUROPEAN ORGANIZATION FOR NUCLEAR RESEARCH
Laboratory for Particle Physics

Departmental Report

CERN/AT 2007-10 (MCS)

ON THE FORMATION OF VOIDS IN INTERNAL TIN Nb_3Sn SUPERCONDUCTORS

C. Scheuerlein[1], M. Di Michiel[2], A. Haibel[3]

In this article we describe three void growth mechanisms in Nb_3Sn strands of the internal tin design on the basis of combined synchrotron micro-tomography and x-ray diffraction measurements during in-situ heating cycles. Initially void growth is driven by a reduction of void surface area by void agglomeration. The main void volume increase is caused by density changes during the formation of Cu_3Sn in the strand. Subsequent transformation of Cu-Sn intermetallics into the lower density α-bronze reduces the void volume again. Long lasting temperature ramps and isothermal holding steps can neither reduce the void volume nor improve the chemical strand homogeneity prior to the superconducting A15 phase nucleation and growth.

1 CERN, Accelerator Technology Department, Geneva, Switzerland
2 European Synchrotron Radiation Facility (ESRF), Grenoble, France
3 Hahn-Meitner Institut Berlin (HMI), Berlin, Germany

To be published in Applied Physics Letters

CERN, Accelerator Technology Department
CH - 1211 Geneva 23
Switzerland

15 March 2007

1 Introduction

The formation of voids during the HT reaction of Nb_3Sn superconductors has been an issue for several decades [1,2]. There is general agreement that it would be beneficial to avoid or at least to control void growth, but the void formation mechanisms and possible remedies to limit void growth remain controversial.

Previous studies of void growth in Nb_3Sn strands have used destructive metallographic techniques. Since the void shape and distribution within Nb_3Sn strands is strongly irregular, metallography results about void formation are erratic and can be strongly misleading. In contrast, by using synchrotron micro-tomography a quantitative description of void volume, shape and distribution can be obtained [3]. Modern synchrotron sources can provide brilliant, high energy x-ray beams, which permit the fast acquisition of tomograms of millimetre thick highly absorbing metallic samples. Due to the short acquisition time of less than a minute per tomogram, tomography experiments during *in-situ* HTs have recently become possible at the ID15A beamline at the European Synchrotron Radiation Facility (ESRF) [4].

In the present article we describe combined tomography and x-ray diffraction measurements during *in-situ* HT of an internal tin (IT) Nb_3Sn strand. The void formation mechanisms are discussed by correlating the quantitative void growth results with the quantitative description of the phase transformations during the HT reaction.

2 Experimental

2.1 The sample

The sample analysed is a Nb_3Sn strand of the IT design, which is described in detail in reference [5].Within the diffusion barrier surrounding the 19 subelements of the strand, the Cu to Sn concentration ratio is approximately 82 wt % Cu and 18 wt % Sn. A metallographic cross section of the Nb_3Sn strand after 1 h at 460 °C is presented in Figure 1.

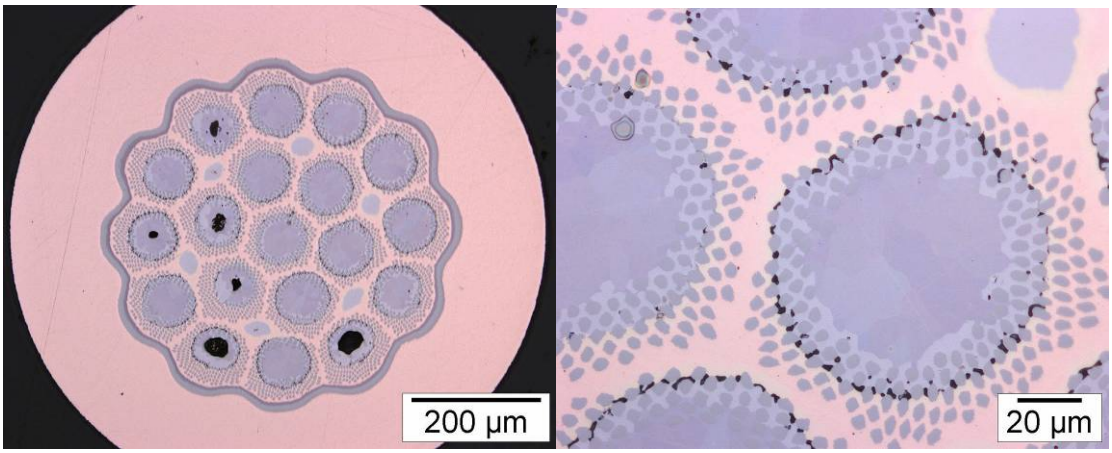

Figure 1: IT Nb_3Sn strand cross section after 460 °C ex-situ HT (ramp rate 6 °C h^{-1}). The black areas in the true colour images are voids. After the 460 °C HT, most of Sn is in the form of Cu_3Sn (dark grey), $Cu_{41}Sn_{11}$ (bright grey) and some α-bronze.

The black areas in the true colour images are voids. One can distinguish between relatively large voids in some of the diffusion centers and voids with sub-µm dimensions, distributed around the filaments at the Cu-Sn intermetallic/α-bronze interface.

2.2 Combined synchrotron tomography and powder diffraction during *in-situ* HT at ID15A

Combined synchrotron micro-tomography and powder diffraction measurements were carried out at the ID15A high energy beamline of ESRF. Absorption micro-tomography was performed using a high intensity filtered white x-ray beam. The tomography set-up is described in detail in [4].

Powder diffraction measurements have been performed in transmission geometry, using a 88.005 keV monochromatic x-ray beam with a bandwidth of 0.1 keV. Debye-Scherrer diffraction pattern were acquired with a MAR 345 image-plate detector. The experiment was optimised for obtaining best possible statistics. The resolution is not sufficient to distinguish between Nb and Ta (lattice constants 3.3066 Å and 3.3058 Å, respectively) and Nb-7.5 wt.%Ta. Cu can not be distinguished from α-bronze.

In-situ heat treatments were performed under inert gas atmosphere (He-H_2 mixture) in a dedicated furnace, which allows both tomographic and diffraction experiments. The accuracy of the sample temperature measurement is better than ±10 °C over the entire temperature range.

3 Results

3.1 Tomography

A 3-D view of the voids present in the diffusion centers of the IT strand at different temperatures is shown in *Figure 2*. The tomograms have been acquired during *in-situ* HT

with a ramp rate of 60 °C h^{-1} with three additional isothermal holding steps for 2 h at 200 °C, 5 h at 340 °C and 2 h at 540 °C.

The first voids are detected in the tomograms at 160 °C. The number of voids, the average void size and the average shape factor (calculated from the ratio void volume to void surface area) increases with increasing temperature. A maximum shape factor of 0.94 is obtained at 200 °C. Isothermal heating at 200 °C and Sn melting at 232 °C influence the void number, volume and shape only slightly. At about 280 °C an elongation of voids, whose diameter is approaching the Sn pool diameter of 50 µm, is observed.

During the 5 h isothermal 340 °C HT the agglomeration of globular voids to larger elongated voids continues. The number of voids detected decreases from 610-330, the average void volume increases from 5.50×10^3 μm^3 to 11.3×10^3 μm^3 and the average void shape factor decreases from 0.92 to 0.75.

At 390 °C the maximum total void volume is obtained and several voids are extending over the entire sampled strand length (1.3 mm). A drastic reduction of total void volume from 5.7×10^6 to 2.5×10^6 μm^3 occurs in the temperature interval 510 to 530 °C.

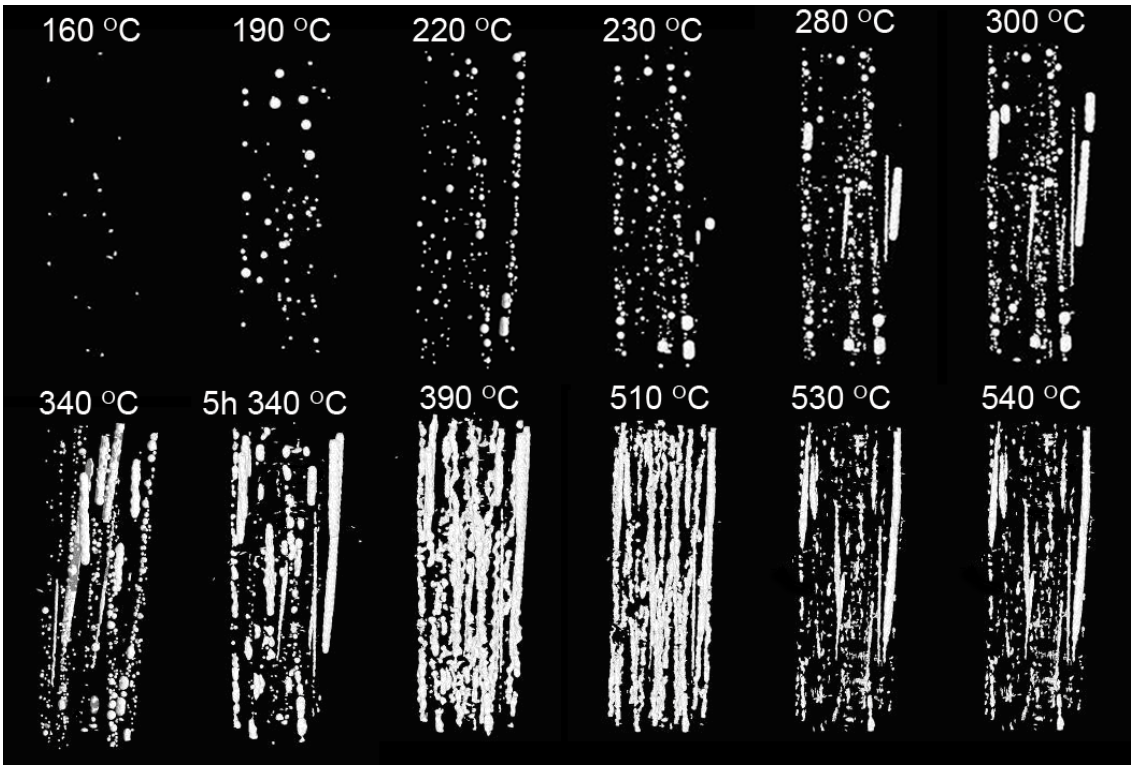

Figure 2: 3-D view of the voids inside the IT strand at different HT temperatures. Binary images have been filtered in order to remove reconstruction artefacts.

During the isothermal 540 °C HT the number of small interfilament voids increases strongly (see Figure 3).

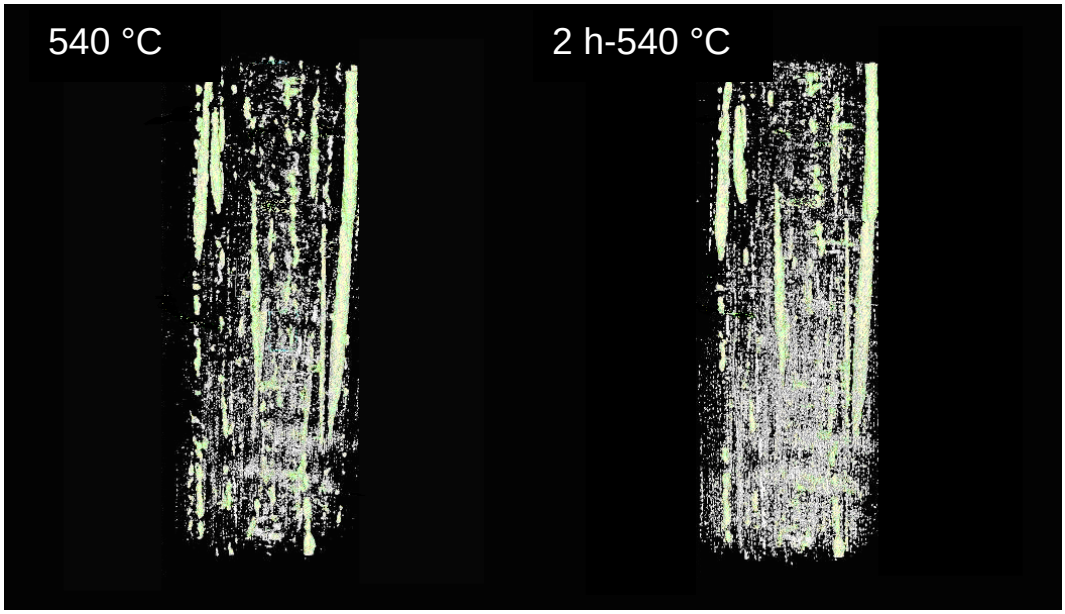

Figure 3: Formation of interfilament voids during isothermal 540 °C HT. The volume of the interfilament voids with diameters in the order of 1 µm can not be measured accurately and only the voids represented in yellow are taken into account in the determination of the void volume within the strand.

3.2 Phase transformations during the reaction HT monitored by *in-situ* x-ray diffraction

During the *in-situ* HT with a ramp rate of 60 °C h^{-1} and isothermal heating for 2 h at 200 °C, 5 h at 340 °C and 5 h at 540 °C, a total of 110 diffractograms were acquired with the position sensitive detector. The 2-D diffraction patterns have been integrated into 1-D diffraction patterns and all are summarised in Figure 4.

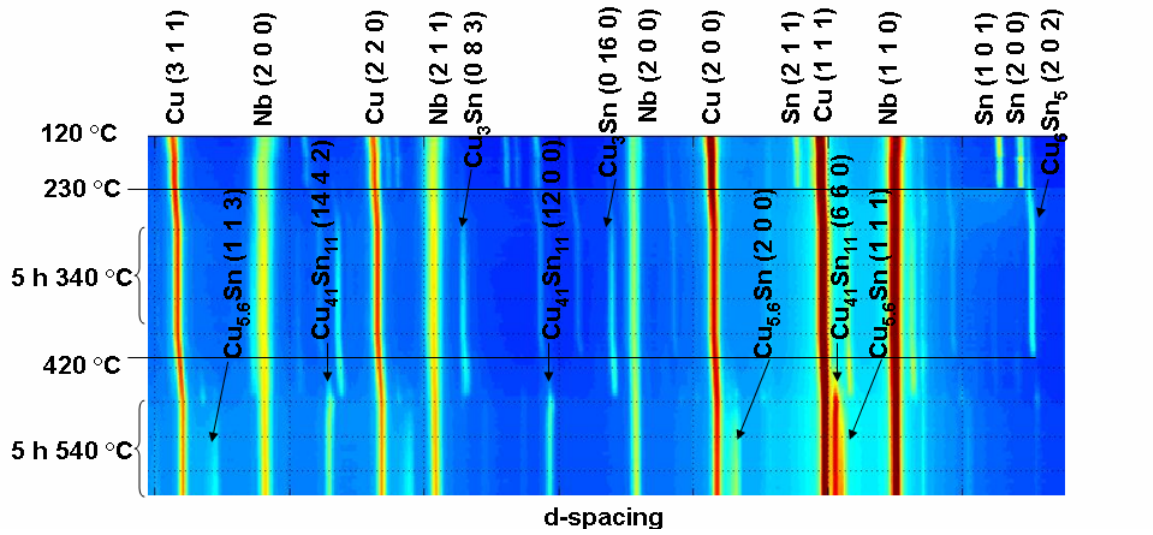

Figure 4: Variation of the diffraction patterns of the IT Nb_3Sn during Cu-Sn mixing HT cycle between 120 °C and 540 °C (ramp rate 60 °C h^{-1}, + isothermal 2 h-200 °C, 5 h-340 °C and 2 h-540 °C HT). Diffractograms have been acquired every 10 minutes.

During the first stage of the HT up to 540 °C, which is often referred to as Cu-Sn mixing HT, five phase transformations are detectable. At first pure Sn and Cu are transformed into Cu_6Sn_5 and Cu_3Sn by solid state diffusion. At around 230 °C the remaining Sn melts. Liquid Sn is present in the strand until 340 °C and vanishes entirely during the 340 °C isothermal holding step. The Cu_6Sn_5 phase continues to grow until at 340 °C it reaches its maximum volume. The Cu_6Sn_5 diffraction peaks decrease strongly in the temperature range 390 °C-410 °C and vanish entirely between 410 °C and 420 °C.

At 430 °C nearly all Sn in the strand is transformed into Cu_3Sn. The Cu_3Sn reflections vanish in the temperature region 500 to 540 °C and at the same time the $Cu_{41}Sn_{11}$ peaks occur. During the isothermal 540 °C HT $Cu_{41}Sn_{11}$ peak intensities decrease and $Cu_{5.6}Sn$ peaks grow. The phase growth results are summarised in Figure 5 and compared with the total void volume inside the strand.

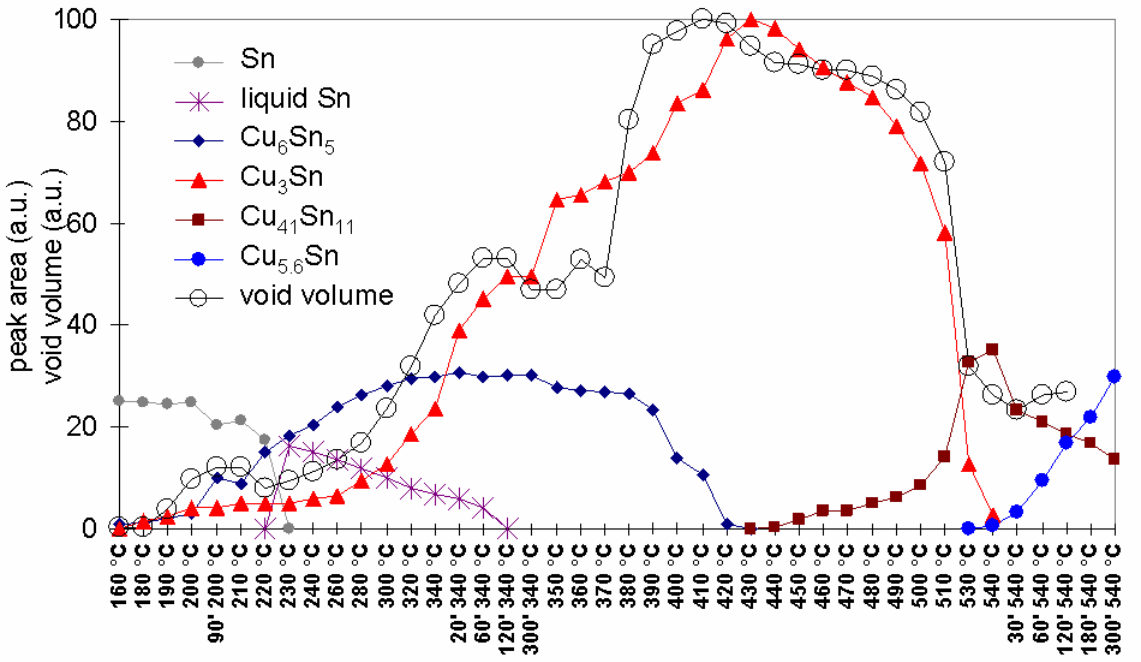

Figure 5: Peak areas of all Sn containing phases, apart from α-bronze, that exist in the IT Nb_3Sn strand during the reaction HT up to 540 °C. The peak areas have been scaled such that the values correspond with the intermetalics volume in the strand. For comparison the total void volume is also shown in the same plot. Void volume is clearly correlated with the Cu_3Sn content in the strand.

The $Cu_{5.6}Sn$ peaks grow until the formation of Nb_3Sn starts at about 580 °C and vanish entirely when the strand is completely reacted (Nb_3Sn growth results are not shown in Figure 4).

4 Discussion

Three different reasons for the formation of voids in IT Nb_3Sn superconductors have been observed.

4.1 Reduction of void surface area through void agglomeration

The growth of the globular voids up to a temperature of about 200 °C is driven by a gain in free energy through a reduction of the total void surface area when smaller voids agglomerate to larger globular voids. It is assumed that voids are already introduced into the Sn during the strand production process used for the studied sample, but they are initially too small to be detected by the tomographic set-up. At 200 °C the maximum ratio of void volume to void surface area is obtained. At this temperature the total void volume (9.6×10^{-5}mm^3) corresponds with 0.14 % of entire strand volume, i.e. 2.5 % of the pure Sn volume.

4.2 Density changes upon intermetallics formation

The densities reported for Cu_6Sn_5, Cu_3Sn and $Cu_{41}Sn_{11}$ exceed the densities of pure (β-) Sn and Cu in the corresponding stoichiometric quantities by 1 %, 4 % [6] and 3 %, respectively. Thus, the metal volume in the diffusion centers shrinks upon Cu-Sn intermetallics formation. Therefore, the void volume increases with Cu_3Sn content in the strand, and the maximum void volume is obtained when Sn is almost entirely transformed into Cu_3Sn (see Figure 5). Afterwards the void volume decreases strongly with increasing temperature until at 540 °C a minimum void volume is obtained. At the same time Cu_3Sn is entirely transformed into the lower density α-bronze and $Cu_{41}Sn_{11}$.

At 390 °C Sn is almost entirely transformed into Cu_3Sn, which occupies 22 vol.% of the sample. The maximum void volume (7.5×10^{-3} mm^3) corresponds with 1.1 % of the sample volume. Thus, assuming a 4 % density increase upon Cu_3Sn formation, the void volume caused by density changes corresponds to 0.90 % of the strand volume.

4.3 Nucleation and growth of Kirkendall voids

During the solid state Cu-Sn interdiffusion there is a generation of vacancies due to differences of the diffusion coefficients of Cu in Sn and Sn in Cu. Under certain conditions the generation of vacancies can cause the nucleation and growth of voids, which are commonly referred to as Kirkendall voids [1,7].

The formation of the relatively small interfilament voids at the Cu-Sn intermetallic/α-bronze interface is assumed to be caused by this effect. As compared to other samples, e.g. Sn solder joints and Sn coatings on Cu substrates [8], the void growth is observed at relatively high temperature, possibly because of stresses in the strand that prevent void growth at lower temperatures.

5 Conclusion

A quantitative description of the void growth and the phase transformations during the HT of an IT Nb_3Sn strand with low Sn content has been obtained. Void growth in IT Nb_3Sn strands is caused by three different mechanisms. The Sn in the non-heat treated strand contains voids that agglomerate during the first HT phase up to 200 °C. Subsequent heating causes void growth through density changes upon intermetallic formation, in particular of Cu_3Sn and the formation of Kirkendall voids. Void growth is

partly reversible when Cu-Sn intermetallics are transformed into the lower density α-bronze.

The influence of so-called isothermal "homogenisation" heat treatments can be assessed from the combined tomography and diffraction results. Isothermal 340 °C heating causes the agglomeration of voids and, thus, reduces the microstructural strand homogeneity. During isothermal 540 °C heating the $Cu_{5.6}Sn$ phase grows and the interfilament void density is increased. Therefore, both isothermal holding steps are counterproductive in improving microstructural and chemical homogeneity.

Acknowledgements

The samples were kindly provided by Alstom-MSA. We are grateful to G. Arnau for EDS measurements and assistance in the phase analysis, and to R. Grupp for technical assistance at the tomography experiments. We also would like to thank L. Oberli and J. Miles for a critical reading of the manuscript.

We acknowledge the ESRF for beam time on ID15A and travel expenses.

One of the authors (C.S.) acknowledges support from the European Community–Research Infrastructure Activity under the FP6 "Structuring the European Research Area" program (CARE, contract number RII3-CT-2003-506395).

References

1 S. Cogan, D.S. Holmes, R.M. Rose, "On the elimination of Kirkendall voids in superconducting composites", Appl. Phys. Lett. 35(7), pp. 557-559, (1979)

2 J.D. Verhoeven, A. Efron, E.D. Gibson, C.C. Cheng, "Void formation in Nb_3Sn-Cu superconducting wire produced by the external tin process", J. Appl. Phys., vol. 59(6), pp. 2105-2113, (1986)

3 A. Haibel, C. Scheuerlein, "Synchrotron tomography for the study of void formation in internal tin Nb_3Sn superconductors", accepted for publication in IEEE Trans. Appl. Supercon.

4 M. Di Michiel, J.M. Merino, D. Fernandez-Carreiras, T. Buslaps, V. Honkimäki, P. Falus, T. Martins, O. Svensson, "Fast microtomography using high energy synchrotron tomography", Rev. Sci. Instrum. 76, 043702, (2005)

5 M. Durante, P. Bredy, A. Devred, R. Otmani, M. Reytier, T. Schild, F. Trillaud, „Development of a Nb_3Sn multifilamentary wire for accelerator magnet applications", *Physica C*, 354, pp. 449-453, (2001)

6 http://www.metallurgy.nist.gov/mechanical_properties/solder_paper.html

7 A. Paul, "The Kirkendall Effect in Solid State Diffusion", PhD Thesis, Technische Universiteit Eindhoven, ISBN 90-386-2646-0, (2004)

8 C. Scheuerlein, Ph. Gasser, P. Jacob, D. Leroy, L. Oberli, M. Taborelli, "The effect of CuSn intermetallics on the interstrand contact resistance in superconducting cables for the Large Hadron Collider", J. Appl. Phys. 97(3), (2005)